LROC NAC Photometry: Preliminary Results and Relative Reflectance of Small Impact Melt Deposits. J. D. Stopar[1], M. S. Robinson[1], B. W. Denevi[2], and S. J. Lawrence[1], [1] School of Earth and Space Exploration, Arizona State University, Tempe AZ, [2] The Johns Hopkins University Applied Physics Laboratory, Laurel MD.

Introduction: Future lunar surface activities will encounter the products of impact processes. Repeat imaging with the Lunar Reconnaissance Orbiter Camera (LROC) Narrow Angle Cameras (NACs) provides a unique dataset taken over a wide range of illumination conditions that can be employed to interpret melt deposit roughness and other surface properties affecting reflectance [e.g., 1-2]. The LROC NACs have already provided sub-meter-scale information on the products and distributions of impact melt deposits including flows, ponds, and veneers [3-6]. In contrast to previous efforts that focused on investigating physical properties of the molten melt [e.g., 3,5], we investigate the reflectance properties of impact melt deposits in their present state as inferred from images taken at different illumination and viewing angles as part of a larger, ongoing analysis.

One of the primary goals of this work is to define parameters that differentiate impact melt deposits, which typically appear to be of lower reflectance than nearby crater deposits [e.g., 7-10], and to determine the cause of this apparent low-reflectance. For example, is glassy melt-rock inherently low-reflectance, do melt-rocks have microscale as well as macroscale roughness [e.g., 2,10-12] that increases shadows and lowers reflectivity, or are the studied melts formed from materials of lower reflectance excavated from the subsurface? The identification of melt products in small, simple craters [e.g., 4-6] – specifically those less than a few hundred meters in diameter that are generally thought too small to exhibit much melt – sometimes relies on relative reflectance in the absence of discernable ponding, cooling fractures, or flow morphologies. However, relative reflectance may not be a unique identifier of impact melt deposits. For example, mature, slumped regolith could contribute to low-reflectance deposits inside craters. Additionally, new, recently formed lunar craters exhibit both low- and high-reflectance ejecta, which have been largely interpreted as changes to near-surface regolith roughness and apparent maturity [13]. Thus, it is imperative that low-reflectance deposits are correctly interpreted, particularly in small, simple craters, to improve our understanding of impact cratering and melting processes.

Data Sources: Repeat imaging of melt deposits over a range of phase, emission, and incidence angles are being acquired as part of the second Lunar Reconnaissance Orbiter (LRO) extended mission. From these observations, we selected three representative young impact craters with impact melt deposits: 1) Baby Ray crater (15.42°E, 9.09°S), a 120-m diameter crater near the Apollo 16 landing site that superposes ejecta from South Ray crater and is characterized by a small low-reflectance area on its floor that could contain melt-rich deposits, but which lacks an obvious ponded morphology. 2) A 3-km diameter crater (49.83°E, 46.75°N) north of Atlas A, with a large low-reflectance deposit extending three crater radii to the NW of the crater rim crest. This low-reflectance deposit was previously interpreted as a veneer of melt-rock based on its occurrence on the crater rim crest and texture [6]. The floor of the parent crater also has a large, asymmetric low-reflectance deposit interpreted as ponded and collected melt with variable surface roughness. And, 3) a ~2.5-km diameter crater southeast of Olcott (121.30°E, 18.68°N) with an asymmetric ejecta distribution, including a low-reflectance ejecta deposit extending to the south from the crater rim. The crater is located on a boundary between terra and mare units. This crater has low-reflectance flows, interpreted as melt deposits [6], extending NW of the crater rim crest for roughly one crater radius, as well as both low- and high-reflectance deposits inside the crater.

For each crater, several measurements of I/F (radiometrically calibrated LROC NAC DN values representing reflectance from images orthorectified using NAC DTMs [14]) were determined for low-reflectance deposits, continuous ejecta, and distal materials. I/F values were measured from the same areas of interest within each overlapping image in order to compare relative reflectivity of melt deposits over a range of illumination and viewing geometries. Only relatively flat, uniform areas were included to minimize topographic effects, and I/F values were normalized to *cos(incidence)cos(emission)*. Additionally, low-to-high phase-ratio images, previously used to investigate roughness differences between parameters [e.g., 2], were generated.

Results and Interpretation:

Baby Ray Crater. Baby Ray crater has a low-reflectance floor with normalized I/F values similar to the "background" material (~6 crater radii from rim crest) across a range of phase angles. The normalized I/F value of the low-reflectance floor deposit is ~45% of that of the continuous ejecta (Fig. 1).

North of Atlas A Crater. Some of the low-reflectance materials on the floor of the crater north of Atlas A, which are interpreted as melt-rich lithologies, have similar normalized I/F values to those of the exte-

rior low-reflectance materials, but other floor materials have reduced normalized I/F in comparison (Fig. 2). The decreased reflectance is correlated with an increase in 1-m and larger blocks and hillocks, suggesting at least a macroscale roughness difference (i.e., shadowing). The smoother (at the m-scale) floor deposits exhibit normalized I/F values that are ~60% of those of the continuous ejecta, nearly the same as the background.

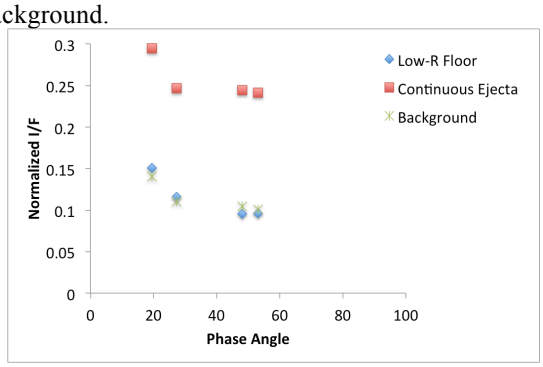

Fig. 1. Phase and normalized I/F for Baby Ray crater deposits.

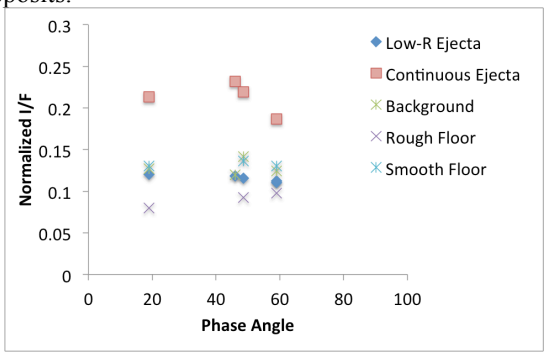

Fig. 2. Phase and normalized I/F for crater deposits north of Atlas A crater.

SE of Olcott Crater. The low-reflectance deposits of the crater located southeast of Olcott (both inside and outside the crater cavity) exhibit normalized I/F values similar to those of the background. The normalized I/F values of the low-reflectance floor deposits are ~50% of those of the continuous ejecta. Higher reflectance floor materials are similar in normalized I/F to those of the continuous ejecta (Fig. 3). Phase-ratios suggest that low-reflectance deposits have variable scattering behaviors (some are more backscattering; others exhibit little change in reflectivity as a function of phase), consistent with previous observations [10].

Discussion and Preliminary Conclusions: On Mercury, the Waters crater low-reflectance "tongue" or flow, also interpreted as an impact melt deposit, is ~11% lower in reflectance relative to the background (at 750-nm), but this contrast varies with phase angle [15]. The lunar deposits described here exhibit normalized melt deposit I/F (panchromatic) values similar to the background (within 5%) across most phase angles. Thus, in many small craters, the apparent low-reflectance deposits may simply be low in reflectance relative to immature, continuous ejecta. Similarities in reflectance between the low-reflectance lunar crater deposits and more distal materials could be a function of maturity, glass content, particle sizes, composition, and/or Fe-reduction of primary minerals during melting and vaporization.

As we proceed, our study will be expanded to include additional craters and deposits, and applying photometric models to our interpretations of roughness and reflectance. We anticipate that our continued photometric investigations of low-reflectance deposits may prove useful in distinguishing melt-rich deposits from other low-reflectance materials based on inferred roughness and scattering behaviors, potentially revealing insights into the cratering processes of small, simple craters.

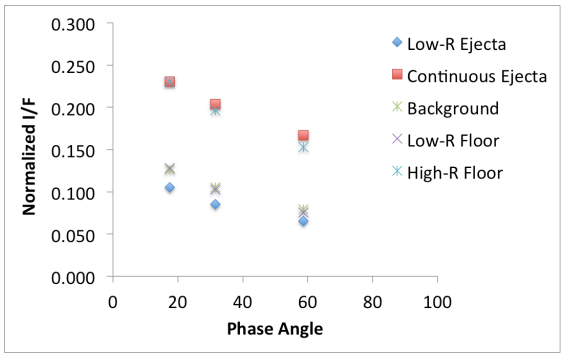

Fig. 3. Phase and normalized I/F for crater deposits southeast of Olcott crater.

References: [1] Clegg R. N. et al. (2014) Icarus, 10.1016/j.icarus.2012.03.020. [2] Shkuratov Y. et al. (2012) Icarus, 10.1016/j.icarus.2011.12.023. [3] Bray V. J. et al. (2010) GRL, 10.1029/2010GL044666. [4] Plescia J. B. and M. J. Cintala (2012) JGR-P, 10.1029/2011JE003941. [5] Denevi B. W. et al. (2012) Icarus, 10.1016/j.icarus.2012.03.020. [6] Stopar J. D. et al. (2014) Icarus, 10.106/j.icarus.2014.08.011. [7] Shoemaker E. M. et al. (1968) in JPL Tech. Rep. 32-1264. [8] Howard K. A. and H. G. Wilshire (1975) in J. Res. USGS 3(2): 237-251. [9] Hawke B. R. and J. W. Head (1977) in Impact Explos. Cratering, pp. 815-841. [10] Wöhler C. et al. (2014) Icarus, 10.1016/j.icarus.2014.03.010. [11] Campbell B. A. et al. (2010) Icarus 208: 565-573. [12] Carter L. M. et al. (2012) JGR-P, 10.1029/2011JE003911. [13] Robinson M. S. et al. (2015) Icarus, 10.1016/ j.icarus. 2015.01.019. [14] Robinson M. S. et al. (2010) Space Sci. Rev., 10.1007/s11214-010-9634-2. [15] Blewett D. T. (2014) Icarus, 10.1016/j.icarus.2014.08.024.